

Research



Cite this article: Hou TY, Shi Z. 2016

Extracting a shape function for a signal with
intra-wave frequency modulation. *Phil. Trans.*

R. Soc. A **374**: 20150194.

<http://dx.doi.org/10.1098/rsta.2015.0194>

Accepted: 29 September 2015

One contribution of 13 to a theme issue
'Adaptive data analysis: theory and
applications'.

Subject Areas:

applied mathematics

Keywords:

sparse time-frequency decomposition,
intra-wave frequency modulation,
shape function

Author for correspondence:

Zuoqiang Shi

e-mail: zqshi@math.tsinghua.edu.cn

Electronic supplementary material is available
at <http://dx.doi.org/10.1098/rsta.2015.0194> or
via <http://rsta.royalsocietypublishing.org>.

Extracting a shape function for a signal with intra-wave frequency modulation

Thomas Y. Hou¹ and Zuoqiang Shi²

¹Applied and Computational Mathematics, MC 9-94, Caltech,
Pasadena, CA 91125, USA

²Mathematical Sciences Center, Tsinghua University, Beijing 100084,
People's Republic of China

In this paper, we develop an effective and robust adaptive time-frequency analysis method for signals with intra-wave frequency modulation. To handle this kind of signals effectively, we generalize our data-driven time-frequency analysis by using a shape function to describe the intra-wave frequency modulation. The idea of using a shape function in time-frequency analysis was first proposed by Wu (Wu 2013 *Appl. Comput. Harmon. Anal.* **35**, 181–199. (doi:10.1016/j.acha.2012.08.008)). A shape function could be any smooth 2π -periodic function. Based on this model, we propose to solve an optimization problem to extract the shape function. By exploring the fact that the shape function is a periodic function with respect to its phase function, we can identify certain low-rank structure of the signal. This low-rank structure enables us to extract the shape function from the signal. Once the shape function is obtained, the instantaneous frequency with intra-wave modulation can be recovered from the shape function. We demonstrate the robustness and efficiency of our method by applying it to several synthetic and real signals. One important observation is that this approach is very stable to noise perturbation. By using the shape function approach, we can capture the intra-wave frequency modulation very well even for noise-polluted signals. In comparison, existing methods such as empirical mode decomposition/ensemble empirical mode decomposition seem to have difficulty in capturing the intra-wave modulation when the signal is polluted by noise.

1. Introduction

Nowadays, data play a more and more important role in our lives. At the same time, the scientific community faces a challenging problem: how to effectively extract useful information from the massive amount of data. In many real-world problems, especially in engineering and physical problems, the frequencies of a signal are usually very useful to help us understand the underlying physical mechanism. Hence, many time-frequency analysis methods have been developed, including the windowed Fourier transform, the wavelet transform [1,2], the empirical mode decomposition (EMD) method [3,4] and the Wigner–Ville distribution [5], to name a few. In particular, the EMD method has found many applications in different disciplines. Inspired by the EMD method, several methods have been proposed in recent years that attempt to provide a mathematical foundation for the EMD method; see, for example, the synchrosqueezed wavelet transform [6,7], the data-driven time-frequency analysis method [8], the empirical wavelet transform [9], the variational mode decomposition [10], the iterative filtering approach [11,12], the approximation method based on short-time Fourier transform [13] and the non-local mean-based method [14].

The data-driven time-frequency analysis method is formulated as a nonlinear optimization problem by looking for the sparsest time-frequency representation of multi-scale data [8]. This is similar in spirit to the compressive sensing [15–17], although we do not know the basis under which the signal has a sparse representation. In this method, the signal is decomposed into several components,

$$f(t) = \sum_{j=1}^M a_j(t) \cos \theta_j(t) + r(t), \quad t \in \mathbb{R}, \quad (1.1)$$

where $a_j(t)$, $\theta_j(t)$ are smooth functions, $\theta'_j(t) > 0$, $j = 1, \dots, M$, and $r(t)$ is a small residual. We assume that $a_j(t)$ and θ'_j are less oscillatory than $\cos \theta_j(t)$. The exact meaning of less oscillatory will be made clear later. We call $a_j(t) \cos \theta_j(t)$ the intrinsic mode functions (IMFs) [3]. This model is widely used in the time-frequency analysis literature under the name adaptive harmonic model [6,13].

One main difficulty in computing the decomposition (1.1) is that the decomposition is not unique. To pick up the ‘best’ decomposition, we proposed to decompose the signal by looking for the sparsest decomposition by solving a nonlinear optimization problem,

$$\left. \begin{array}{l} \text{minimize} \quad M \\ (a_k)_{1 \leq k \leq M}, (\theta_k)_{1 \leq k \leq M} \\ \text{subject to:} \quad f = \sum_{k=1}^M a_k \cos \theta_k + r(t), \quad a_k \cos \theta_k \in \mathcal{D}, \end{array} \right\} \quad (1.2)$$

where \mathcal{D} is the dictionary consisting of all IMFs (see [8] for its precise definition).

To solve (1.2), we proposed two algorithms. The first one is based on matching pursuit [8] and the other one is based on basis pursuit [18]. In a subsequent paper [19], the authors proved the convergence of the nonlinear matching pursuit algorithm for periodic data that satisfy a certain scale separation property.

Although model (1.1) has been applied to a number of applications with success and the decomposition methods have been shown to be effective and efficient, there are also some applications such as the Stokes waves or some nonlinear dynamic systems for which our methods do not work well. Figure 1 gives one example of the Stokes wave. In the Stokes wave, comparing with the cosine wave, the trough is flatter and the crest is sharper, which implies that the instantaneous frequency is small near the trough and large near the crest. Thus, the instantaneous frequency of the Stokes wave has one cycle within one wave cycle, which means that the instantaneous frequency is as oscillatory as the original wave. For those signals whose instantaneous frequency is as oscillatory as or even more oscillatory than the original wave, we call them signals with intra-wave frequency modulation [20]. It is observed that the intra-wave

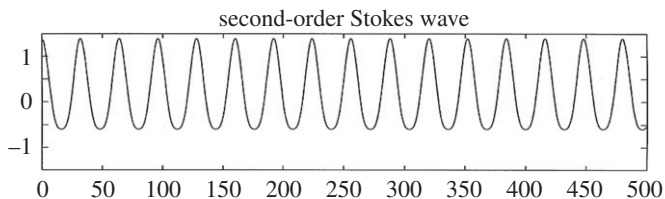


Figure 1. One example of signals with intra-wave modulation: Stokes wave. (Adapted from [3].)

frequency modulation is very common in some nonlinear dynamic systems and this is also closely related to the nonlinear feature of the underlying physical system [3,20]. The intra-wave modulation can reveal the nonlinear feature of a signal. The EMD method can be used to compute the intra-wave frequency modulation for signals without noise. However for signals with noise, the EMD (or ensemble empirical mode decomposition (EEMD)) method tends to give artificial harmonic waves rather than a wave with intra-wave frequency modulation, since the EMD (or EEMD) acts essentially as a dyadic filter bank for Gaussian noise [4,21,22]. One of the main purposes of this paper is to develop an efficient and robust method to compute the intra-wave modulation of a signal even when it is corrupted by noise.

Unfortunately, the model we used before (1.1) does not work well for signals with intra-wave modulation. The reason for this is that our previous method requires that the instantaneous frequencies are less oscillatory than the signal. Therefore, this method cannot compute the instantaneous frequency with intra-wave modulation.

Inspired by the idea of introducing a shape function in [23], we can develop an alternative way to capture the intra-wave modulation by introducing a shape function to replace the cosine function in model (1.1). The key observation is that the intra-wave modulation can be absorbed into a shape function which captures the essential wave pattern of the signal. For example, in the Stokes wave shown in figure 1, the shape function should be a cosine-like function with a flat trough and a sharp crest. After introducing the shape function which absorbs all intra-wave modulation, the amplitude and the instantaneous frequency remain smooth. This enables us to develop a more efficient numerical algorithm that is stable to noise perturbation.

By incorporating the idea of a shape function into our previous model (1.1), we get the following model:

$$f(t) = \sum_{k=1}^M a_k(t) s_k(\theta_k(t)) + r(t), \quad (1.3)$$

where s_k is an unknown 2π -periodic ‘shape function’ which is adapted to the signal. The envelope $a_k(t)$ and the phase function $\theta_k(t)$ are smooth functions and are less oscillatory than $s(\theta_k(t))$. We also assume that $\theta'_k(t) > 0$.

With the introduction of the shape function, the model has more degrees of freedom, which makes the problem more difficult to solve. To simplify the problem, in this paper, we only consider those signals that have one dominated shape function, i.e. $M = 1$ in (1.3). By exploring the fact that the shape function is a periodic function of the phase function, θ , we can identify a certain low-rank structure of the signal. This structure enables us to extract the shape function from the signal.

We remark that, in the model with the shape function, all intra-wave modulation is captured by the shape function. The amplitude function $a(t)$ and the phase function remain as smooth functions, which means that they have only inter-wave modulation. If we adopt the definition of the degree of nonlinearity from Huang *et al.* in [20], only the intra-wave modulation contributes to the degree of nonlinearity. In this sense, the essential nonlinear feature of the signal is encoded in the shape function. The amplitude and the phase function in the model using the shape function would have no contribution to the degree of nonlinearity.

We would like to emphasize that we can recover the instantaneous frequency with intra-wave modulation in the original EMD method once the shape function is obtained. One advantage of this approach is that the instantaneous frequency with intra-wave modulation obtained from the shape function is very stable to noise perturbation. Using this approach, we can capture the intra-wave frequency modulation very well even for noise-polluted signals. In comparison, some existing methods such as the EMD/EEMD seem to have difficulty in capturing the intra-wave modulation when the signal is polluted by noise. The EMD method is known to be unstable to noise perturbation. Although the EEMD method is more stable to noise perturbation, the instantaneous frequencies obtained by the EEMD tend to be smoothed out by the ensemble averaging process as demonstrated in the example of the Duffing equations. As a consequence, the EEMD does not capture very well the strong intra-wave frequency modulation in comparison with the original EMD method for noise-free signals.

The rest of this paper is organized as follows. In §2, the decomposition model for data with intra-wave frequency modulation is presented. The details of the algorithm and the localized version are given in §§3 and 4. We present some numerical results in §5. Some concluding remarks are made in §6.

2. Models for a signal with intra-wave frequency modulation

In order to design a computational algorithm for model (1.3), we first need to define the meaning of ‘less oscillatory’. To simplify the discussion, in this section, we assume that the signal is periodic. We will discuss general non-periodic signals in §4. With a given phase function $\theta(t)$, we construct a linear space $V(\theta, \lambda)$ which is spanned by the following basis:

$$\left\{ \left(\cos \left(\frac{k\theta}{L_\theta} \right) \right), \left(\sin \left(\frac{k\theta}{L_\theta} \right) \right) \right\}_{0 \leq k \leq \lambda L_\theta}, \quad (2.1)$$

where $\lambda < 1/2$ is a parameter to control the smoothness of functions in $V(\theta, \lambda)$, $L_\theta = (\theta(1) - \theta(0))/2\pi$ is a positive integer and $[0, 1]$ is the range of the signal in time. And we require $a_k(t)$ and $\theta'_k(t)$ to be $V(\theta_k, \lambda)$ to enforce that they are less oscillatory than $\cos \theta_k$. In this paper, we choose $\lambda = 1/2$ and, in the rest of the paper, we drop λ in $V(\theta, \lambda)$ to simplify the notation.

Then, the model of the signal is given as follows:

$$f(t) = \sum_{k=1}^M a_k(t) s_k(\theta_k(t)) + r(t), \quad a_k, \theta'_k \in V(\theta_k) \text{ and } \theta'_k > 0, \quad s_k \text{ is } 2\pi\text{-periodic}. \quad (2.2)$$

Corresponding to this model, we propose to solve the following optimization problem to find the sparsest decomposition (2.2):

$$\left. \begin{array}{l} \min_{a_k, \theta_k, s_k} \quad M \\ \text{subject to:} \quad \sum_{k=1}^M a_k s_k(\theta_k) + r(t) = f, \quad a_k s_k(\theta_k) \in \mathcal{M}, \end{array} \right\} \quad (2.3)$$

where the dictionary \mathcal{M} is defined as

$$\mathcal{M} = \{ a_k s_k(\theta_k) : a_k, \theta'_k \in V(\theta_k), \theta'_k > 0, s_k \text{ is a } 2\pi\text{-period function.} \} \quad (2.4)$$

This optimization problem is very difficult to solve. In this paper, we focus on a simpler case. We assume that the signal is dominated by one component in \mathcal{M} , i.e.

$$f(t) = a(t) s(\theta(t)) + r(t), \quad a, \theta' \in V(\theta), \text{ and } \theta' > 0, \quad s \text{ is } 2\pi\text{-periodic}. \quad (2.5)$$

Here, $r(t)$ is the residual. The residual $r(t)$ could be noise or a trend or some kind of perturbation. No matter what $r(t)$ is, we assume that it is small in amplitude compared with $a(t)s(\theta(t))$.

Using the idea of matching pursuit, the decomposition in (2.5) can be obtained by solving the following optimization problem:

$$\min_{a, \theta, s} \|f(t) - a(t)s(\theta(t))\|_2^2, \quad \text{subject to: } a(t)s(\theta(t)) \in \mathcal{M}. \quad (2.6)$$

Although this optimization problem is much simpler than (2.3), it is still very difficult to solve. It is highly nonlinear. The envelope a , the phase function θ and the shape function s are all unknown. They are all adaptive to the data. This feature makes our method fully adaptive to the signal, but it also introduces additional difficulty to solve the resulting optimization problem (2.6).

Inspired by our previous work in the data-driven time-frequency analysis [8], we develop an efficient method to solve (2.6). This method consists of two steps. First, the smooth phase function is computed by our data-driven time-frequency analysis [8].

Since s is periodic, it can be represented by the Fourier basis,

$$s(t) = \sum_{k=-K}^K c_k e^{ikt} = b_0 + \sum_{k=1}^K (b_k \cos(kt) + d_k \sin(kt)), \quad (2.7)$$

where $b_k = \text{Re}(c_k)$, $d_k = -\text{Im}(c_k)$ and $k = 0, \dots, K$. In the above Fourier series representation, we assume that s is K -band limited, which is a good approximation as long as s is smooth enough and K is large enough. Then the signal $f(t)$ can be written as follows:

$$\begin{aligned} f(t) &= a(t)s(\theta(t)) + r(t) \\ &= b_0 a(t) + a(t) \sum_{k=1}^K (b_k \cos(k\theta(t)) + d_k \sin(k\theta(t))) + r(t) \\ &= b_0 a(t) + \sum_{k=1}^K \left(a(t) \sqrt{b_k^2 + d_k^2} \right) \cos(k\theta(t) + \phi_k) + r(t), \end{aligned} \quad (2.8)$$

where $\phi_k = \arctan(d_k/b_k)$.

From the above derivation, $f(t)$ can be seen as a signal composed by K IMFs with instantaneous frequency $k\theta'(t)$, respectively. Note that the instantaneous frequencies, $k\theta'(t)$, are well separated without intersections, which means that the signal f satisfies the scale separation property. Then, we could use the method developed in [8] to compute its phase function. We refer to [8] for the details of the algorithm.

From the representation (2.8), we can also see another advantage of the model with shape function. All the artificial harmonic waves are absorbed to the shape function. This enables us to obtain a sparse representation of the signal.

Once the phase function is obtained, by exploring the fact that s is a periodic function of θ , we can identify certain low-rank structure of the signal. This structure enables us to extract the shape function from the signal. The details will be given in the next section.

3. An efficient algorithm to compute the shape function

The phase function θ has been obtained in the previous section, then the optimization problem (2.6) can be reduced to the following problem:

$$\min_{a, s} \|f(t) - a(t)s(\theta(t))\|_2^2, \quad \text{subject to: } a \in V(\theta), \quad s(\cdot) \text{ is } 2\pi\text{-periodic.}$$

Using the Fourier series representation of the shape function (2.7), the optimization problem becomes

$$\min_{a, c_k} \left\| f - a \sum_{k=-K}^K c_k e^{ik\theta} \right\|_2^2, \quad \text{subject to: } a \in V(\theta).$$

Next, in order to further simplify the above optimization problem, we replace the standard l^2 norm in the objective function to the l^2 norm in the θ -space,

$$\|f\|_{2,\theta} = \left(\int_0^{2\pi} f^2 d\bar{\theta} \right)^{1/2} = \left(\int_0^1 f^2(t) \bar{\theta}'(t) dt \right)^{1/2},$$

where $\bar{\theta} = \theta/L_\theta$ is the normalized phase function which is used as the coordinate function in the θ -space and $L_\theta = (\theta(1) - \theta(0))/2\pi$. In this paper, we assume that the signal lies in $[0, 1]$.

Then, the above optimization problem is reduced to

$$\min_{a, c_k} \left\| \sum_{\omega=-\infty}^{+\infty} \hat{f}_\theta(\omega) e^{i\omega\theta/L_\theta} - a \sum_{k=-K}^K c_k e^{ik\theta} \right\|_{2,\theta}^2, \quad \text{subject to: } a \in V(\theta), \quad (3.1)$$

where \hat{f}_θ is the Fourier coefficients of f in the θ -space,

$$\hat{f}_\theta(\omega) = \int_0^1 f(t) e^{-i\omega\bar{\theta}(t)} \bar{\theta}'(t) dt.$$

Next, we represent the envelope a by the Fourier basis in the θ -space,

$$a = \sum_{\omega=-\infty}^{+\infty} \hat{a}_\theta(\omega) e^{i\omega\bar{\theta}}.$$

Then we have

$$\begin{aligned} a \sum_{k=-K}^K c_k e^{ik\theta} &= \sum_{k=-K}^K c_k \left(\sum_{\omega=-\infty}^{+\infty} \hat{a}_\theta(\omega) e^{i(\omega+kL_\theta)\bar{\theta}} \right) \\ &= \sum_{k=-K}^K c_k \left(\sum_{\omega=-\infty}^{+\infty} \hat{a}_\theta(\omega - kL_\theta) e^{i\omega\bar{\theta}} \right) \\ &= \sum_{\omega=-\infty}^{+\infty} \left(\sum_{k=-K}^K c_k \hat{a}_\theta(\omega - kL_\theta) \right) e^{i\omega\bar{\theta}}. \end{aligned}$$

Then, (3.1) becomes

$$\min_{\hat{a}_\theta, c_k} \left\| \sum_{\omega=-\infty}^{+\infty} \left[\hat{f}_\theta(\omega) - \sum_{k=-K}^K c_k \hat{a}_\theta(\omega - kL_\theta) \right] e^{i\omega\bar{\theta}} \right\|_{2,\theta}^2 \quad \text{subject to: } a \in V(\theta).$$

Using the well-known Parseval identity, the objective function is equal to the l^2 norm of the Fourier coefficients, which gives rise to the following equivalent optimization problem:

$$\min_{\hat{a}_\theta, c_k} \sum_{\omega=-\infty}^{+\infty} \left| \hat{f}_\theta(\omega) - \sum_{k=-K}^K c_k \hat{a}_\theta(\omega - kL_\theta) \right|^2, \quad \text{subject to: } a \in V(\theta).$$

Since $a \in V(\theta)$, using the definition of $V(\theta)$, we have $\hat{a}_\theta(\omega) = 0$, $|\omega| \geq L_\theta/2$. Then we get

$$\begin{aligned} \sum_{\omega=-\infty}^{+\infty} \left| \hat{f}_\theta(\omega) - \sum_{k=-K}^K c_k \hat{a}_\theta(\omega - kL_\theta) \right|^2 &= \sum_{j=-\infty}^{+\infty} \sum_{\omega=-L_\theta/2}^{L_\theta/2-1} \left| \hat{f}_\theta(\omega + jL_\theta) - \sum_{k=-K}^K c_k \hat{a}_\theta(\omega + (j-k)L_\theta) \right|^2 \\ &= \sum_{j=-K}^K \sum_{\omega=-L_\theta/2}^{L_\theta/2-1} |\hat{f}_\theta(\omega + jL_\theta) - c_k \hat{a}_\theta(\omega)|^2 \\ &\quad + \sum_{\substack{|j|>K, \\ j \in \mathbb{Z}}} \sum_{\omega=-L_\theta/2}^{L_\theta/2-1} |\hat{f}_\theta(\omega + jL_\theta)|^2, \end{aligned}$$

where we have used the fact that, if $k \neq j$, $\hat{a}_\theta(\omega + (j-k)L_\theta) = 0$ for any $-L_\theta/2 \leq \omega < L_\theta/2$ in obtaining the last equality.

Using the above derivation, we have the following equivalent optimization problem:

$$\min_{\hat{a}_\theta, c_k} \sum_{k=-K}^K \sum_{|\omega| < L_\theta/2} |\hat{f}_\theta(\omega + kL_\theta) - c_k \hat{a}_\theta(\omega)|^2.$$

Denote

$$\hat{f}_{\theta,k}(\omega) = \begin{cases} \hat{f}_\theta(\omega), & kL_\theta \leq \omega < (k+1)L_\theta, \\ 0, & \text{otherwise} \end{cases}$$

and

$$f_{\theta,k}(\bar{\theta}) = \mathcal{F}_\theta^{-1}(\hat{f}_{\theta,k}(\omega))(\bar{\theta}) = \sum_{\omega=-\infty}^{+\infty} \hat{f}_{\theta,k}(\omega) e^{i\omega\bar{\theta}}.$$

Then, using the Parseval identity one more time, we need only to solve the following equivalent problem:

$$\min_{a_\theta, c_k} \sum_{k=-K}^K \|f_{\theta,k}(\bar{\theta}) - c_k a_\theta(\bar{\theta})\|_2^2, \quad (3.2)$$

where $a_\theta(\bar{\theta}(t)) = a(t)$ is the representation of a in the θ -space. Fortunately, after discretization, the above optimization problem can be solved by the singular value decomposition (SVD).

Suppose a_θ and $f_{\theta,k}$ is sampled over $\bar{\theta}_j = (j-1)/N$, ($j=1, \dots, N$), which is a uniform grid in the $\bar{\theta}$ -space. Let

$$\mathbf{f}_{\theta,k} = (f_{\theta,k}(\bar{\theta}_1), \dots, f_{\theta,k}(\bar{\theta}_N))^t, \quad (3.3)$$

$$\mathbf{F}_\theta = (\text{Re}(\mathbf{f}_{\theta,0}), \dots, \text{Re}(\mathbf{f}_{\theta,K}), \text{Im}(\mathbf{f}_{\theta,1}), \dots, \text{Im}(\mathbf{f}_{\theta,K})) \quad (3.4)$$

and

$$\mathbf{a}_\theta = (a_\theta(\bar{\theta}_1), \dots, a_\theta(\bar{\theta}_N))^t, \quad (3.5)$$

$$\mathbf{c} = (\text{Re}(c_0), \dots, \text{Re}(c_K), \text{Im}(c_1), \dots, \text{Im}(c_K)). \quad (3.6)$$

Then, the discrete version of (3.2) is

$$\min_{\substack{\mathbf{c} \in \mathbb{R}^{2K+1} \\ \mathbf{a}_\theta \in \mathbb{R}^N}} \|\mathbf{F}_\theta - \mathbf{a}_\theta \cdot \mathbf{c}\|_{\mathbb{F}}^2, \quad (3.7)$$

where $\|\cdot\|_{\mathbb{F}}$ is the Frobenius norm of a matrix. It is well known that the above optimization problem can be solved by SVD.

Suppose

$$\mathbf{F}_\theta = \mathbf{U} \cdot \mathbf{S} \cdot \mathbf{V}$$

is the SVD of \mathbf{F}_θ , $\text{diag}(\mathbf{S}) = (s_1, \dots, s_{2K+1})$ and $s_1 \geq s_2 \geq \dots \geq s_{2K+1} \geq 0$. Then the solution of the optimization problem (3.7) is

$$\mathbf{a}_\theta = \mathbf{u}_1, \quad \mathbf{c} = \mathbf{v}_1, \quad (3.8)$$

where \mathbf{u}_1 is the first column of matrix \mathbf{U} and \mathbf{v}_1 is the first row of matrix \mathbf{V} .

Summarizing the above discussion, we obtain algorithm 1 to compute the shape function with a given phase function.

Algorithm 1. (Extraction of a shape function).

Input: Signal $\mathbf{f} = (f(t_1), \dots, f(t_N))$ is sampled over $t_l, l = 1, \dots, N$, the phase functions θ , and the band width of shape function K .

Output: The shape function s and the corresponding envelope $a(t)$.

- 1: Interpolate the original signal \mathbf{f} from $t_l, l = 1, \dots, N$ to a uniform grid $\bar{\theta}_j = j/N, j = 0, \dots, N - 1$ in the $\bar{\theta}$ -space.

$$f_{\theta}^j = \text{interpolate}(\theta(t_l), f(t_l), \bar{\theta}_j).$$

In the computation, we use the cubic spline to do the interpolation.

- 2: Compute the Fourier coefficients of f in the θ -space

$$\hat{f}_{\theta}(\omega) = \sum_{j=0}^{N-1} f_{\theta}^j e^{-i\omega\bar{\theta}_j}, \quad \omega = -\frac{N}{2}, \dots, \frac{N}{2} - 1.$$

- 3: Compute $f_{\theta,k}, k = 0, \dots, K$,

$$f_{\theta,k}(\bar{\theta}_j) = \sum_{\omega=(k-1/2)L_{\theta}}^{(k+1/2)L_{\theta}-1} \hat{f}_{\theta}(\omega) e^{i\omega\bar{\theta}_j}.$$

- 4: Assemble the matrix \mathbf{F}_{θ} according to (3.4).
- 5: Apply SVD on \mathbf{F}_{θ} to get the envelope $a_{\theta}(\bar{\theta}_j), j = 1, \dots, N$ and $c_k, k = 0, \dots, K$ according to (3.5), (3.6) and (3.8).
- 6: Compute the shape function and the envelope function in the t -space

$$s(t_l) = \sum_{k=-K}^K c_k e^{ikt_l}, \quad l = 1, \dots, N,$$

$$a(t_l) = \text{interpolate}(\bar{\theta}_j, a_{\theta}(\bar{\theta}_j), \theta(t_l)),$$

where $c_{-k} = c_k^*$ is the complex conjugate of c_k . The interpolation is also implemented by the cubic spline.

4. The signal with varying shape function

For non-stationary signals, the shape function may change over time. In many applications, it is important to characterize the changing of the shape function, which could reveal the physical mechanism under the signal. In [24], inspired by the concept of the degree of nonlinearity which was proposed by Huang *et al.* [20], we assume that the shape function of the signal is governed by a second-order ordinary differential equation (ODE) with polynomial nonlinearity. Then we formulated an optimization problem to calculate the coefficients of the ODE. The coefficients of the second-order ODE are used to describe the changing of the shape function. Using these techniques, we can see clearly how the shape function changes and detect the time when significant change occurs. In order to apply this method to detect the changing of the shape function, we need to develop one local method to extract the ‘instantaneous’ shape function, which is the main purpose of this section.

The idea we use here is straightforward. First, we cut the whole signal into a number of small pieces and apply the method proposed in the previous section to obtain the shape function in each piece. Then we can get a series of shape functions which could show us how the shape function varies.

Suppose we have a signal $\mathbf{f} = (f(t_1), \dots, f(t_N))$ which is sampled at t_1, \dots, t_N , and the phase function $\theta = (\theta(t_1), \dots, \theta(t_N))$ is also given. For each t_m , $m = 1, \dots, N$, we want to use the signal around t_m to get a shape function.

First, we extract a small piece of signals \mathbf{f}_m and the phase function θ_m around t_m , the length of \mathbf{f}_m depends on the phase function θ ,

$$\mathbf{f}_m = \mathbf{f}_T \chi_T \quad \text{and} \quad \theta_m = \theta_T,$$

where $\mathbf{f}_T = (f(t_j))_{j \in T}$ and $\theta_T = (\theta(t_j))_{j \in T}$. Here, $T = \{1 \leq j \leq N : |\theta(t_j) - \theta(t_m)| \leq \mu\pi\}$ and

$$\chi_T = \left(\frac{1}{2} \left(1 + \cos \left(\frac{t_j}{\mu} \right) \right) \right)_{j \in T}.$$

Here, μ is a parameter to control the length of the segment. In this paper, we choose $\mu = 3$, which means that, for each point, we localize the signal within three local periods to extract the shape function.

Once we get the segments \mathbf{f}_m and θ_m , the shape function can be obtained by using the method described in the previous section. For each t_m , repeat this process; then we get a series of shape functions which could capture the change of the shape function.

5. Numerical results

In this section, we will present some numerical results to demonstrate the performance of our algorithm.

Example 5.1. The first example is a simple synthetic signal which is generated by the following formula:

$$\theta(t) = 40\pi t + 2 \cos(6\pi t), \quad (5.1)$$

$$a(t) = \frac{1}{2 + \sin(2\pi t)} \quad (5.2)$$

and

$$f(t) = \frac{a(t)}{1.1 + \cos[\theta(t) + \cos(2\theta(t))]} \quad (5.3)$$

From the phase function, $\theta(t) + \cos(2\theta(t))$ in (5.3), it is clear that the signal has intra-wave frequency modulation. If we do not insist that the shape function must be a cosine function, then the phase function becomes θ given in (5.1), which is much smoother than $f(t)$, and the shape function $s(t)$ has the form $1/(1.1 + \cos(t + \cos 2t))$. In figure 2, the shape function given by our method is shown. As we can see, our method could capture the shape function very accurately. Next, we add Gaussian noise, $0.3X(t)$, to the clean signal to test the robustness of our method. $X(t)$ is the standard Gaussian noise with zero mean and variance $\sigma^2 = 1$. The result is shown in figure 3. Even with noise, our method still recovers the shape function with reasonable accuracy.

Example 5.2 (Duffing equation). In the second example, the signal is given by the solution of the Duffing equation. We use this example to demonstrate the importance of the intra-wave frequency modulation in some complex dynamical system.

The Duffing equation is a nonlinear ODE which has the following form:

$$\frac{d^2u}{dt^2} + u + \epsilon u^d = \gamma \cos(\beta t), \quad (5.4)$$

where ϵ is a small parameter, γ is the amplitude of the driving force and β is the basic frequency of the driving force.

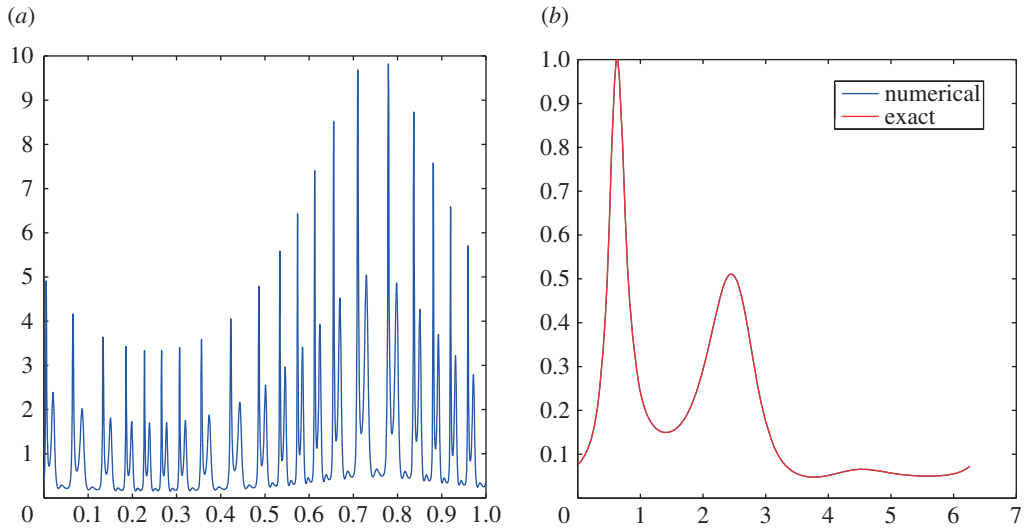


Figure 2. (a) The original data in example 5.1. (b) The shape function obtained by our method (blue) and the exact shape function (red). (Online version in colour.)

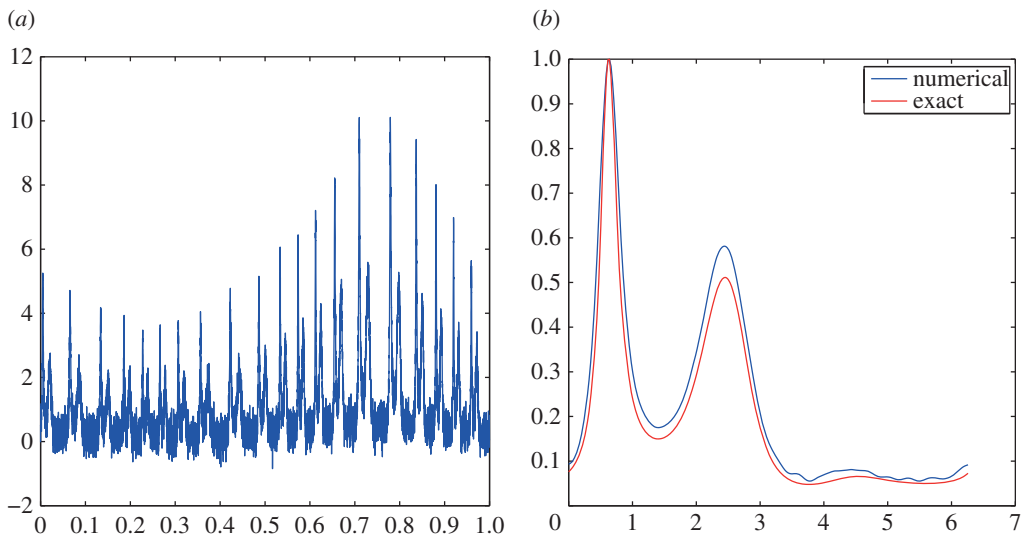


Figure 3. (a) The noise data $f(t) + 0.3X(t)$, where $f(t)$ is given in example 5.1 and $X(t)$ is the white noise with standard derivative $\sigma^2 = 1$. (b) The shape function obtained by our method (blue) and the exact shape function (red). (Online version in colour.)

The Duffing equation can be solved by a perturbation method (e.g. [25]). The solution is expressed as a series in terms of the small parameter ϵ as follows:

$$u(t) = u_0(t) + \epsilon u_1(t) + \epsilon^2 u_2(t) + \dots \quad (5.5)$$

Substituting the series (5.5) into the original equation (5.4), we can obtain the equations for $u_j(t)$, $j=0,1,2,\dots$, by matching the coefficients of different order of ϵ . To simplify the

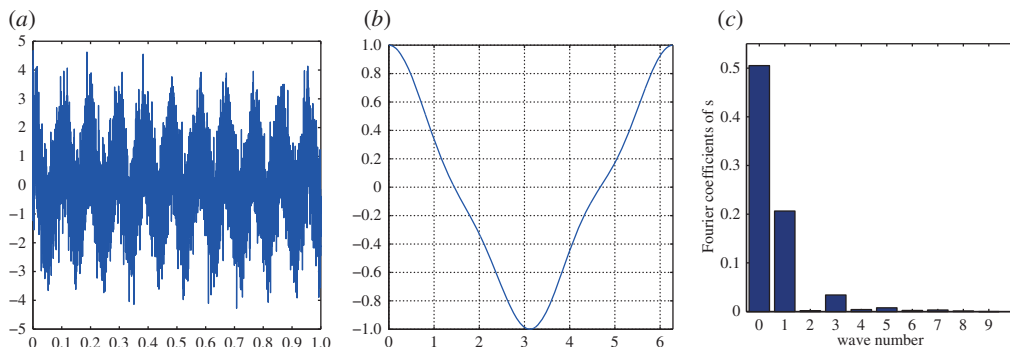


Figure 5. (a) The solution of the Duffing equation with noise $X(t)$; (b) the shape function s ; and (c) the Fourier coefficients of s . (Online version in colour.)

from the noisy signal still retains the main characteristics of the shape function extracted from the signal without noise.

As we can see from figure 4, when the solution is not polluted by noise, the Fourier coefficient of the shape function is almost 0 for the wavenumber $k=2$. From the previous discussion, this actually implies that $d=3$ in the Duffing equation if we know that the signal comes from an ODE of the form given in (5.4). When the solution is corrupted by noise, as shown in figure 5, the Fourier coefficient at $k=2$ is also much smaller than the Fourier coefficients at $k=1$ and $k=3$, which strongly suggests that $d=3$ in the original Duffing equation. This phenomenon may be very special, but it suggests that some quantities, such as the deviation of the Fourier coefficients of the shape function, may reflect some important feature of the underlying physical system. This idea is similar in spirit to the definition of the degree of nonlinearity introduced by Huang *et al.* in [20]. They used the deviation of the instantaneous frequency to quantify the degree of nonlinearity,

$$\text{DN} = \left\langle \left(\frac{\text{IF} - \text{IF}_z}{\text{IF}_z} \right)^2 \right\rangle^{1/2}, \quad (5.9)$$

where IF stands for the instantaneous frequency, IF_z stands for the constant mean frequency over one wave cycle and $\langle \cdot \rangle$ denotes the average over one wave cycle.

Actually, the deviation of the instantaneous frequency is closely related to the Fourier coefficients of the shape function. When the Fourier coefficients are concentrated at $k=1$, there is no intra-wave frequency modulation, which implies that the degree of nonlinearity is zero. If the shape function has large Fourier coefficients at $k \neq 1$, the intra-wave modulation of the instantaneous frequency is also very large; in that case, the degree of nonlinearity would be large.

This example shows that the shape function may contain a key feature that characterizes the degree of nonlinearity of a signal. In this paper, we just make this observation. Whether or not this observation is true for more general data still requires further investigation. The shape function captures a certain key nonlinear feature of the signal. The discussion of the degree of nonlinearity based on the shape function will appear in our subsequent paper. In the current paper, we will focus on the computation of the shape function.

Actually, in this example, the instantaneous frequency with intra-wave modulation could be recovered from the shape function. After the normalization to make $\max s = 1$ and $\min s = -1$, we can express $s(t)$ in terms of $\cos \phi(t)$ by taking

$$\phi(t) = \arccos(s(t)).$$

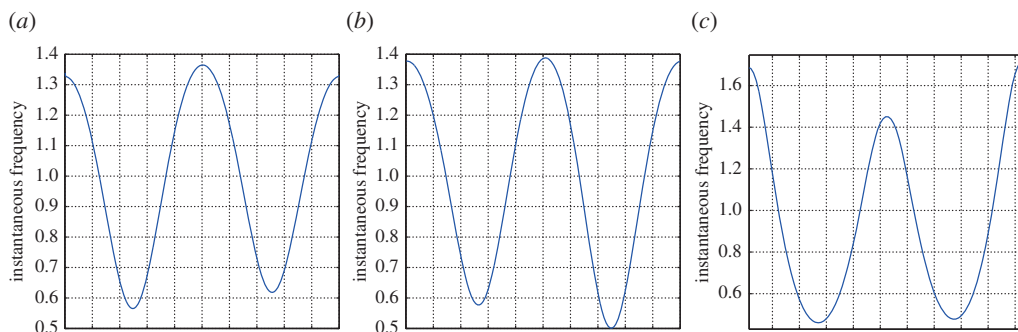


Figure 6. (a) The instantaneous frequency recovered from the shape function for the solution of the Duffing equation; (b) the instantaneous frequency recovered from the shape function for the solution of the Duffing equation with noise; and (c) the instantaneous frequency given by the EMD for the noise-free solution in one wave cycle. (Online version in colour.)

From the phase function ϕ , we can recover the instantaneous frequency with intra-wave modulation by defining the instantaneous frequency as

$$IF^s = \frac{d\phi(t)}{dt} = \phi'(t).$$

By adopting the definition of the degree of nonlinearity in (5.9), we have the following definition of the degree of nonlinearity with the instantaneous frequency recovered from the shape function:

$$DN^s = \left(\frac{1}{2\pi} \int_0^{2\pi} \left(\frac{\phi'(\tau) - \bar{\phi}'}{\bar{\phi}'} \right)^2 d\tau \right)^{1/2},$$

where $\bar{\phi}' = (1/2\pi) \int_0^{2\pi} \phi'(\tau) d\tau$.

We remark that the instantaneous frequency, IF^s , recovered from the shape function is not exactly the same as the instantaneous frequency in the EMD method, since, in IF^s , only the intra-wave modulation is taken into account; in the EMD method, the instantaneous frequency includes both the intra-wave and inter-wave modulation. The difference can be clearly seen in figure 6. However, these two instantaneous frequencies actually give an equivalent degree of nonlinearity, as shown in appendix A. The reason for this is that in the definition of the degree of nonlinearity, (5.9), the inter-wave modulation is actually factored out. This fact also shows that the nonlinearity is encoded in the shape function, while the amplitude and instantaneous frequency have no contribution to the nonlinearity if the definition of the degree of nonlinearity given by Huang *et al.* is adopted.

In figure 6a,b, we give the instantaneous frequencies recovered from the shape function for the solution without and with noise in one wave cycle. As we can see, they both have very strong intra-wave modulation. And even with a large noise perturbation to the solution of the Duffing equation, we can still get the instantaneous frequency that captures the main feature of the underlying Duffing equation. For the noise-free signal, the EMD method could also capture the intra-wave frequency modulation, as shown in figure 6c. The instantaneous frequency obtained from the shape function is not the same as that obtained by the EMD method. The difference between the instantaneous frequencies obtained by the two methods is due to the fact that the inter-wave modulation is not included in the shape function; see appendix A for a detailed explanation.

When the signal is polluted by noise, the EMD/EEMD methods seem to have difficulty in capturing the intra-wave frequency modulation. In figure 7, the IMFs obtained by the EMD/EEMD for the noise-free signal and the noisy signal are shown. When the signal is free of noise, we can see that there is a sharp cusp-like pattern near the crests and the troughs of

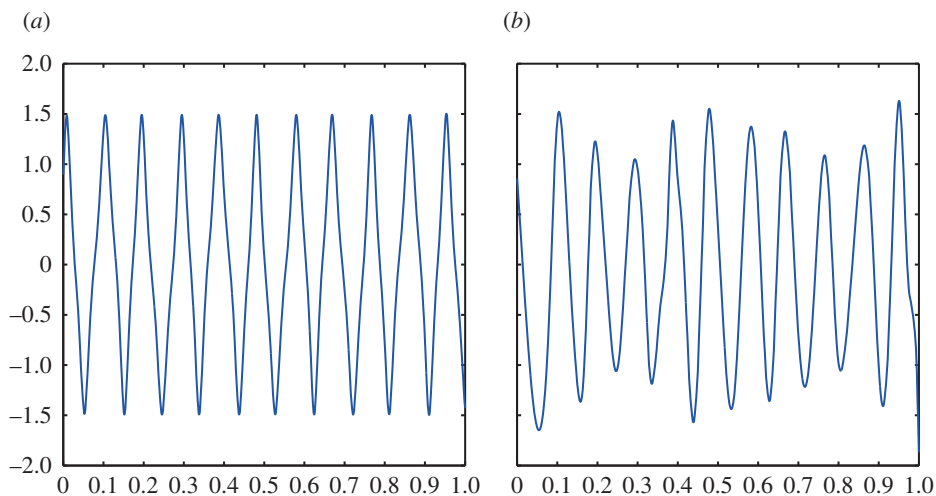


Figure 7. The IMFs given by the EMD/EEMD in the noise-free case (a) and the noisy case (b). (Online version in colour.)

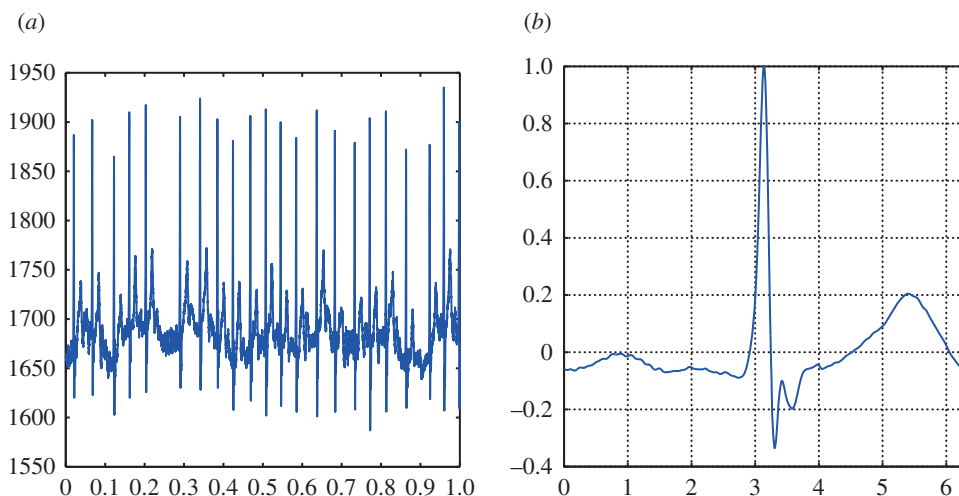


Figure 8. (a) The original electrocardiogram (ECG) data and (b) the shape function obtained by our method for the ECG data. (Online version in colour.)

the wave. Such a pattern is responsible for the strong intra-wave modulation of the solution, as shown in figure 6c. However, for the IMF extracted from the noisy signal by the EEMD method, such a sharp pattern near the crests and the troughs of the wave is smoothed out. As a result, the intra-wave frequency modulation is significantly reduced. On the other hand, our method based on the shape function still gives the instantaneous frequency with intra-wave modulation, as shown in figure 6b.

Example 5.3 (ECG data). In this example, we consider a section of electrocardiogram (ECG) data. The length of the data used here is 16 s. Figure 8a shows the shape function extracted from this set of ECG signals. We remark that it is challenging to extract the shape function from ECG data since the data have sharp peaks in each period. This means that the shape function is not regular and needs many Fourier coefficients to represent it accurately. The shape function that we

have extracted seems to have all the characteristics of a typical ECG period. The interpretation of the significance of the shape function requires expertise in medicine and is beyond the scope of this paper.

6. Concluding remarks

In this paper, we present an efficient and robust method to extract the shape function from signals with intra-wave frequency modulation by exploiting the intrinsic low-rank structure of the data. This method works only for those signals with one dominating shape function. Extracting shape functions for signals with multiple shape functions is much more involved and requires more effort. Once the shape function is obtained, we can recover the instantaneous frequency with intra-wave modulation. We would like to emphasize that the instantaneous frequency obtained from the shape function is very stable to noise perturbation. As a consequence, we can capture the intra-wave frequency modulation very well even for noise-polluted signals. In comparison, some existing methods such as the EMD/EEMD seem to have difficulty in capturing the strong intra-wave frequency modulation for noisy signals. The Fourier coefficients of the shape function seem to contain important information regarding the degree of nonlinearity of the signal. Since our method of extracting the shape function is quite stable with respect to noise perturbation, one can potentially use the Fourier coefficients of the shape function to give an alternative definition of the degree of nonlinearity of a signal, as done by Huang *et al.* in [20]. Further studies in this direction will be reported in our future work.

Data accessibility. Data in examples 5.1 and 5.2 are synthetic data. They can be reproduced following the descriptions in the paper. Data used in example 5.3 can be found in the electronic supplementary material.

Authors' contributions. Both authors, T.Y.H. and Z.S., worked together to propose the proper formulation for this problem. Z.S. carried out most of the work in the design and the implementation of the numerical algorithms. He also drafted the manuscript. T.Y.H. revised the manuscript and ensured that a thorough study of the proposed method was carried out. Both authors gave final approval for publication.

Competing interests. The authors declare that they have no competing interests.

Funding. This work was supported by NSF FRG grant nos. DMS-1159138, DMS-1318377; AFOSR MURI grant no. FA9550-09-1-0613; and DOE grant no. DE-FG02-06ER25727. The research of Z.S. was supported by NSFC grant no. 11201257.

Appendix A. Degree of nonlinearity

Consider an IMF with a constant amplitude $a(t) = 1$. Let $\theta^E(t)$ be the phase function in the EMD method and $\theta^S(t)$ be the corresponding phase function in the model with the shape function. We assume that the shape function has been normalized so that its amplitude is bounded by 1, i.e. $\max_t s(t) = 1$ and $\min_t s(t) = -1$. Denote $\phi(t) = \arccos(s(t))$.

Using the fact that both $\cos \theta^E(t)$ and $s(\theta^S(t))$ are the representations of the same signal, we have

$$\cos \theta^E(t) = s(\theta^S(t)),$$

which implies that

$$\theta^E(t) = \phi(\theta^S(t)).$$

Thus, the instantaneous frequency in the original EMD method can be computed as follows:

$$\text{IF} = \frac{d}{dt} \theta^E(t) = \phi'(\theta^S(t))(\theta^S)'(t), \quad (\text{A } 1)$$

and the mean frequency over one wave cycle, IF_z , becomes

$$\text{IF}_z = \frac{1}{T} \int_{t_0}^{t_1} \phi'(\theta^S(t))(\theta^S)'(t) dt,$$

where the time interval $[t_0, t_1]$ contains one wave cycle and $T = t_1 - t_0$. Then we have $\theta^S(t_1) - \theta^S(t_0) = 2\pi$, which gives that

$$IF_z = \frac{1}{T} \int_0^{2\pi} \phi'(\tau) d\tau.$$

Using the fact that θ^S is a smooth function which is approximately a constant over one wave cycle, it follows that

$$[(\theta^S)'(t)]T \approx \theta^S(t_1) - \theta^S(t_0) = 2\pi, \quad \forall t \in [t_0, t_1].$$

Using the above approximation, we get

$$IF_z \approx (\theta^S)'(t) \left(\frac{1}{2\pi} \int_0^{2\pi} \phi'(\tau) d\tau \right). \quad (\text{A } 2)$$

Recall that the degree of nonlinearity is defined as

$$\text{DN} = \left\langle \left(\frac{IF - IF_z}{IF_z} \right)^2 \right\rangle^{1/2}.$$

Substituting (A 1) and (A 2) into the above definition, we have

$$\text{DN} = \left\langle \left(\frac{IF - IF_z}{IF_z} \right)^2 \right\rangle^{1/2} \approx \left\langle \left(\frac{\phi'(\theta^S(t)) - \bar{\phi}'}{\bar{\phi}'} \right)^2 \right\rangle^{1/2} \approx \left(\frac{1}{2\pi} \int_0^{2\pi} \left(\frac{\phi'(\tau) - \bar{\phi}'}{\bar{\phi}'} \right)^2 d\tau \right)^{1/2},$$

where $\bar{\phi}' = (1/2\pi) \int_0^{2\pi} \phi'(\tau) d\tau$.

This formal derivation shows that using the instantaneous frequency recovered from the shape function actually gives an equivalent definition of the degree of nonlinearity by using the shape function.

References

1. Daubechies I. 1992 *Ten lectures on wavelets*. CBMS-NSF Regional Conference Series on Applied Mathematics, no. 61. Philadelphia, PA: SIAM Publications.
2. Mallat S. 2009 *A wavelet tour of signal processing: the sparse way*. New York, NY: Academic Press.
3. Huang NE *et al.* 1998 The empirical mode decomposition and the Hilbert spectrum for nonlinear and non-stationary time series analysis. *Proc. R. Soc. Lond. A* **454**, 903–995. (doi:10.1098/rspa.1998.0193)
4. Wu Z, Huang NE. 2009 Ensemble empirical mode decomposition: a noise-assisted data analysis method. *Adv. Adapt. Data Anal.* **1**, 1–41. (doi:10.1142/S1793536909000047)
5. Flandrin P. 1999 *Time-frequency/time-scale analysis*. San Diego, CA: Academic Press.
6. Daubechies I, Lu J, Wu H. 2011 Synchrosqueezed wavelet transforms: an empirical mode decomposition-like tool. *Appl. Comp. Harmon. Anal.* **30**, 243–261. (doi:10.1016/j.acha.2010.08.002)
7. Thakur G, Wu HT. 2011 Synchrosqueezing-based recovery of instantaneous frequency from nonuniform samples. *SIAM J. Math. Anal.* **43**, 2078–2095. (doi:10.1137/100798818)
8. Hou TY, Shi Z. 2013 Data-driven time-frequency analysis. *Appl. Comput. Harmon. Anal.* **35**, 284–308. (doi:10.1016/j.acha.2012.10.001)
9. Gilles J. 2013 Empirical wavelet transform. *IEEE Trans. Signal Process* **61**, 3999–4010. (doi:10.1109/TSP.2013.2265222)
10. Dragomiretskiy K, Zosso D. 2014 Variational mode decomposition. *IEEE Trans. Signal Process* **62**, 531–544.
11. Lin L, Wang Y, Zhou H. 2009 Iterative filtering as an alternative for empirical mode decomposition. *Adv. Adapt. Data Anal.* **1**, 543–560. (doi:10.1142/S179353690900028X)
12. Huang C, Yang L, Wang Y. 2009 Convergence of a convolution-filtering-based algorithm for empirical mode decomposition. *Adv. Adapt. Data Anal.* **1**, 561–571.
13. Chui CK, Mhaskar HN. 2015 Signal decomposition and analysis via extraction of frequencies. *Appl. Comput. Harmon. Anal.* **40**, 97–136. (doi:10.1016/j.acha.2015.01.003)

14. Galiano G, Velasco J. 2014 On a non-local spectrogram for denoising one-dimensional signals. *Appl. Math. Comput.* **244**, 1–13. (doi:10.1016/j.amc.2014.06.092)
15. Candes E, Romberg J, Tao T. 2006 Robust uncertainty principles: exact signal recovery from highly incomplete frequency information. *IEEE Trans. Inform. Theory* **52**, 489–509. (doi:10.1109/TIT.2005.862083)
16. Candès E, Tao T. 2006 Near optimal signal recovery from random projections: universal encoding strategies? *IEEE Trans. Inform. Theory* **52**, 5406–5425. (doi:10.1109/TIT.2006.885507)
17. Donoho DL. 2006 Compressed sensing. *IEEE Trans. Inform. Theory* **52**, 1289–1306. (doi:10.1109/TIT.2006.871582)
18. Hou TY, Shi Z. 2014 Sparse time-frequency decomposition by dictionary learning. (<http://arxiv.org/abs/1311.1163>)
19. Hou TY, Shi Z, Tavallali P. 2014 Convergence of a data-driven time-frequency analysis method. *Appl. Comput. Harmon. Anal.* **37**, 235–270. (doi:10.1016/j.acha.2013.12.004)
20. Huang NE *et al.* In preparation. On the degree of nonlinearity for oscillatory systems.
21. Flandrin P, Rilling G, Gonçalves P. 2004 Empirical mode decomposition as a filter bank. *IEEE Signal Process. Lett.* **11**, 112–114. (doi:10.1109/LSP.2003.821662)
22. Wu Z, Huang NE. 2004 A study of the characteristics of white noise using the empirical mode decomposition method. *Proc. R. Soc. Lond. A* **460**, 1597–1611. (doi:10.1098/rspa.2003.1221)
23. Wu H-T. 2013 Instantaneous frequency and wave shape functions (I). *Appl. Comput. Harmon. Anal.* **35**, 181–199. (doi:10.1016/j.acha.2012.08.008)
24. Hou TY, Shi Z, Tavallali P. 2013 Sparse time frequency representations and dynamical systems. *Commun. Math. Sci.* **13**, 673–694. (doi:10.4310/CMS.2015.v13.n3.a4)
25. Drazin PG. 1992 *Nonlinear systems*. Cambridge, UK: Cambridge University Press.